Thromboxane A2 receptor and MaxiK-channel intimate interaction supports channel *trans*-inhibition independent of G-protein activation

Min Li[a], Yoshio Tanaka[b], Abderrahmane Alioua[a], Yong Wu[a], Rong Lu[a], Pallob Kundu[a,1], Enrique Sanchez-Pastor[a,2], Jure Marijic[a], Enrico Stefani[a,c,d,3], and Ligia Toro[a,d,e,3,4]

Departments of [a]Anesthesiology, [e]Molecular and Medical Pharmacology, and [c]Physiology, and [d]Brain Research Institute, University of California, Los Angeles, CA 90095; and [b]Department of Chemical Pharmacology, School of Pharmaceutical Sciences, Toho University, Funabashi, Chiba 274-8510, Japan

Edited by David E. Clapham, Children's Hospital Boston, The Howard Hughes Medical Institute, Boston, MA, and approved September 16, 2010 (received for review March 2, 2010)

Large conductance voltage- and calcium-activated potassium channels (MaxiK, BK_{Ca}) are well known for sustaining cerebral and coronary arterial tone and for their linkage to vasodilator β-adrenergic receptors. However, how MaxiK channels are linked to counterbalancing vasoconstrictor receptors is unknown. Here, we show that vasopressive thromboxane A2 receptors (TP) can intimately couple with and inhibit MaxiK channels. Activation of the receptor with its agonist *trans*-inhibits MaxiK independently of G-protein activation. This unconventional mechanism is supported by independent lines of evidence: (*i*) inhibition of MaxiK current by thromboxane A2 mimetic, U46619, occurs even when G-protein activity is suppressed; (*ii*) MaxiK and TP physically associate and display a high degree of proximity; and (*iii*) Förster resonance energy transfer occurs between fluorescently labeled MaxiK and TP, supporting a direct interaction. The molecular mechanism of MaxiK–TP intimate interaction involves the receptor's first intracellular loop and C terminus, and it entails the voltage-sensing conduction cassette of MaxiK channel. Further, physiological evidence of MaxiK–TP physical interaction is given in human coronaries and rat aorta, and by confirming TP role (with antagonist SQ29,548) in the U46619-induced MaxiK inhibition in human coronaries. We propose that vasoconstrictor TP receptor and MaxiK-channel direct interaction facilitates G-protein–independent TP to MaxiK *trans*-inhibition, which would promote vasoconstriction.

BK_{Ca} channel | G-protein–coupled receptor | Smooth muscle

Vascular tone results from a balance between vasoconstricting and vasodilatory forces acting in response to changes in metabolism. Much work has been focused on the vasorelaxing role of large conductance voltage- and calcium-activated potassium channels (MaxiK, BK_{Ca}). In this context, MaxiK channels are activated by vasorelaxants like β-adrenergic agents via channel coupling to β-adrenergic receptors and Gs protein (1–3). In fact, β-adrenergic receptors have been found to associate with MaxiK channels (4). However, little attention has been paid to study the relationship between MaxiK channels and vasoconstrictor receptors.

The potent vasoconstrictor thromboxane A2, aside from being released from platelets in pathological situations (favoring thrombosis and vasospasm), is also produced in smooth muscle, underscoring its possible contribution to the normal contractile responses of arterial myocytes. We first published that MaxiK channels from pig coronary smooth muscle reconstituted into lipid bilayers could be inhibited by the thromboxane A2 analog, U46619 (5). In these studies, the action of U46619 did not require the presence of GTP and Mg^{2+}, suggesting a process independent of G-protein activation and a tight molecular coupling between the receptor and the channel proteins. However, reconstitution experiments may not fully represent the mechanisms used by proteins in their native environment. We now show in living cells that thromboxane A2 receptors (TP) and MaxiK channels form a regulatory complex, and provide evidence for a TP-to-MaxiK direct inhibitory mechanism that is independent of G-protein activation. Further, we identify the protein domains in TP and MaxiK responsible for their physical association.

Results

Thromboxane A2 Receptor and the Pore-Forming α-Subunit of MaxiK Channel Form a Macromolecular Complex. To investigate the potential association of human TP and the pore-forming α-subunit of the human MaxiK channel (named here MaxiK), we first performed coimmunoprecipitation experiments in HEK293T cells transiently expressing MaxiK (expected mass ~125 kDa) and N-terminal c-Myc–tagged TP (c-Myc–TP, expected mass ~39 kDa). Fig. 1*A* shows that immunoprecipitation of c-Myc–TP pulls down MaxiK (lane 3, $n = 6$). Likewise, reverse coimmunoprecipitation showed that MaxiK is also able to pull down TP (Fig. 1*B*, lane 3; $n = 3$). Negative controls with only one protein expressed showed no MaxiK (Fig. 1*A*, lanes 1 and 2) or TP signals (Fig. 1*B*, lanes 1 and 2). Positive controls show that TP (Fig. 1*C*) and MaxiK (Fig. 1*D*) were effectively immunoprecipitated. Also, no immunoprecipitation of TP or MaxiK were observed in mock-transfected cells (Fig. 1 *C* and *D*, lane 1). The immunoblots of the corresponding lysates confirmed proper expression of all clones (Fig. 1 *E* and *F*).

The specificity of TP–MaxiK association was further confirmed by mixing lysates from cells independently overexpressing MaxiK or TP. In this case, MaxiK and TP could not be coimmunoprecipitated, ruling out the possibility that the association observed in lysates of coexpressing cells could result from random protein–protein interactions of overexpressed proteins (Fig. S1).

To determine whether TP and MaxiK associate at the plasma membrane, we performed live labeling of HEK293T cells coexpressing N-terminal–tagged Flag-TP and c-Myc–MaxiK. Confocal images of live-labeled cells show a high level of TP and MaxiK overlap along the plasma membrane (Fig. 1 *G–I*). To quantify their degree of colocalization, we calculated their protein proximity index (6) (Fig. S2). Fig 1*J* is the cross-correlation 3D plot of Fig. 1 *G* and *H* as a function of pixel shift. At zero pixel shift, the surface plot has a peak that decays abruptly by shifting the image a few pixels, indicative of specific colocalization. The mean protein proximity index values were for TP→MaxiK, 0.64 ± 0.11, and for MaxiK→TP, 0.77 ± 0.13 (Fig. 1*K*; $n = 22$ cells). Confirming a close proximity, a line scan

Author contributions: M.L., Y.T., A.A., R.L., P.K., E.S.-P., E.S., and L.T. designed research; M.L., Y.T., and J.M. performed research; Y.W. and E.S. contributed new reagents/analytic tools; M.L., Y.T., and E.S. analyzed data; and M.L. and L.T. wrote the paper.

The authors declare no conflict of interest.

This article is a PNAS Direct Submission.

[1]Present address: Plant Molecular and Cellular Genetics Section, Bose Institute, Kolkata, West Bengal 700 054, India.

[2]Present address: Centro Universitario de Investigaciones Biomédicas, Universidad de Colima, Colima, 28045, Mexico.

[3]E.S. and L.T. contributed equally to this work as senior authors.

[4]To whom correspondence should be addressed. E-mail: ltoro@ucla.edu.

This article contains supporting information online at www.pnas.org/lookup/suppl/doi:10.1073/pnas.1002685107/-/DCSupplemental.

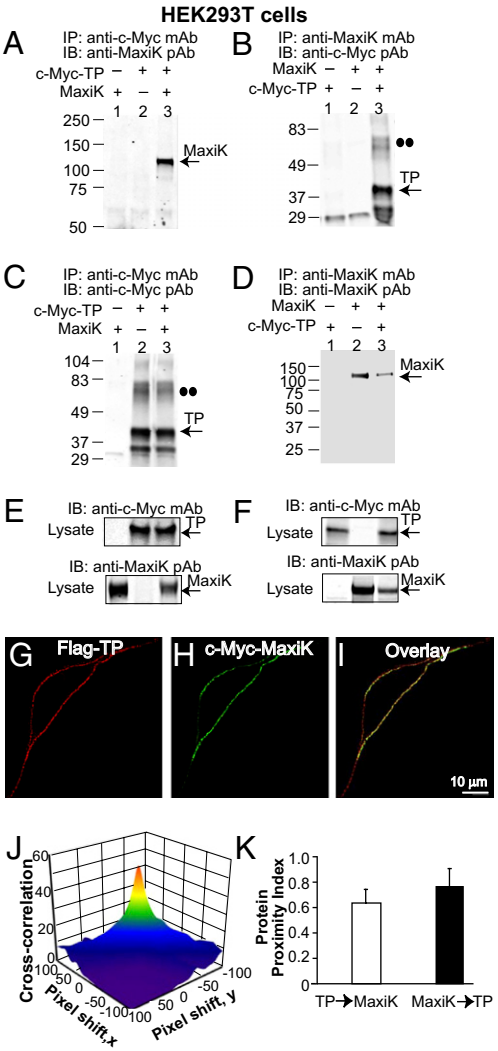

Fig. 1. Association of TP with MaxiK in cotransfected HEK293T cells. (*A*) c-Myc–TP pulls down MaxiK. (*B*) MaxiK pulls down c-Myc-TP. Double dots (*B* and *C*) mark the TP dimer. (*C* and *D*) Positive controls showing corresponding TP and MaxiK immunoprecipitation. (*E* and *F*) Double-labeled immunoblots of input lysates (10 μg protein/lane). (*G* and *H*) Nonpermeabilized HEK293T cell expressing Flag–TP and c-Myc–MaxiK. Cells were live immunolabeled with anti-Flag monoclonal (red) and anti–c-Myc polyclonal (green) antibodies. (*I*) Superimposed confocal images. Images are single planes at the middle of the cell. (*J*) 3D plot of TP and MaxiK cross-correlation vs. pixel shift. (*K*) Mean protein proximity index values showing TP–MaxiK high degree of proximity. In this and following figures, numbers at the left of immunoblots correspond to molecular masses in kilodaltons, and antibodies used for immunoprecipitation (IP) and immunoblots (IB) are given at the margins of each blot. pAb, polyclonal antibody; mAb, monoclonal antibody.

through the plasma membrane also gives a high degree of correlation (0.68; Fig. S3). The above protein proximity index values are in close agreement with those shown later in native myocytes, confirming the specific TP and MaxiK association after ectopic expression.

TP and MaxiK Coexist Within a 6-nm Distance. To explore whether the association of TP and MaxiK channel may occur via a direct protein–protein interaction, we performed Förster resonance energy transfer (FRET) experiments. HEK293T cells were cotransfected with MaxiK–CFP + TP–YFP C-terminal fusion fluorescent proteins. As positive control, we transfected cells with CFP linked to YFP via a 6-aa (DPPVAT) random linker (CFP-linker-YFP). As negative controls, we used: (*i*) nonlinked CFP + YFP, (*ii*) MaxiK–CFP + YFP, and (*iii*) CFP + TP–YFP; in these cases, any signals would originate from random FRET due to overexpression and nonspecific protein interactions. Fig. 2 *A* and *B* shows that only MaxiK–CFP + TP–YFP and the positive control CFP-linker-YFP displayed significant normalized FRET (*SI Materials and Methods*). The normalized FRET for MaxiK–CFP + TP–YFP at the cell periphery was 0.53 ± 0.11 ($n = 18$), whereas for CFP-linker-YFP was 0.78 ± 0.09 ($n = 13$), but in this case and as expected for a soluble protein, the signal was homogenously distributed within the cell. In contrast, for negative controls, the normalized FRET signal was rather small (CFP + YFP = 0.22 ± 0.10, $n = 13$) or negligible (MaxiK–CFP + YFP = 0.04 ± 0.08, $n = 11$, and CFP + TP–YFP = 0.03 ± 0.03, $n = 9$).

To confirm FRET between MaxiK–CFP and TP–YFP and to calculate the energy transfer efficiency and distance between molecules, the photobleaching method was applied (*SI Materials and Methods*). Photobleaching TP–YFP caused a significant decrease of net FRET when compared with control (Fig. 2*D* vs. Fig. 2*C*). Conversely, a significant increase of MaxiK–CFP fluorescence was observed after photobleaching the cell (Fig. 2*F* vs. Fig. 2*E*), as excited MaxiK–CFP was no longer able to transfer energy to TP–YFP. Graphs in Fig. 2 *G* and *H* correspond to the line scans of images in Fig. 2 *C*–*F* and show the loss of net FRET and gain of MaxiK–CFP signal after photobleaching (black lines). The mean value of MaxiK–CFP to TP–YFP energy transfer efficiency at the cell periphery was 0.30 ± 0.07, and the calculated distance between MaxiK and TP was 5.7 ± 0.3 nm ($n = 5$). In summary, both FRET quantification methods show that MaxiK-CFP and TP-YFP proteins specifically interact and are in close contact within a 6-nm distance.

TP-to-MaxiK Coupling via a Mechanism Independent of G-Protein Activation. G proteins play an essential role in transducing the stimulation of G-protein–coupled receptors (GPCRs) to downstream effector proteins, including ion channels. Given the fact that in bilayers, TP-mediated MaxiK inhibition did not require GTP supplementation (5), and that TP and MaxiK are in close contact in intact cells as learned from FRET experiments, we questioned whether their functional coupling required G-protein activation. To address this point, we recorded MaxiK currents at 6.7 μM Ca^{2+} from HEK293T cells coexpressing MaxiK + TP and used as a pharmacological tool, GDPβS. GDPβS inhibits G-protein activation by locking Gα in its inactive state and preventing the exchange with GTP. To stimulate TP, we perfused U46619—a stable analog of thromboxane A2—to the intracellular side of inside-out patches; U46619 is lipophilic and was able to reach its binding site on the extracellular face of TP. Fig. 3*A* shows that perfusion of bath solution alone (perfusion control) had no significant effect on MaxiK currents, whereas perfusion of 500-nM U46619 inhibited current activity, as observed by the slowdown in activation kinetics and reduced tail currents at the beginning of negative test pulses. Instantaneous tail currents (measured at the beginning of the −70 mV repolarizing pulses) were used to construct mean fractional open probability (Po) vs. membrane potential curves. U46619 caused a shift of ~30 mV in the half-activation potential, $V_{1/2}$, from -9.6 ± 9.3 in control to 18.7 ± 8.8 mV (Fig. 3*B*; $n = 5$). Supporting a G-protein-independent mechanism, 500-μM GDPβS was unable to prevent U46619-induced inhibition (Fig. 3 *C* and *D* vs. *A* and *B*). A similar $V_{1/2}$ shift of ~30 mV as with U46619 alone was observed (control = -8.5 ± 12.9 mV; GDPβS + U46619 = 19.1 ± 14.0 mV; $n = 4$). As controls, GDPβS alone did not have a significant effect on channel currents (Fig. 3 *C* and *D*), and U46619 did not have an effect when MaxiK was transfected alone ($n = 6$; Fig. S4). Moreover, the activity of GDPβS was tested in parallel experiments where GDPβS effectively blocked the inhibitory action of GTP + Mg^{2+} on Kir2.2 whole-cell currents ($n = 4$; Fig. S5). Therefore, the lack of GDPβS action on U46619-induced MaxiK inhibition indicates that TP is able to regulate MaxiK channel in the absence of G-protein activation.

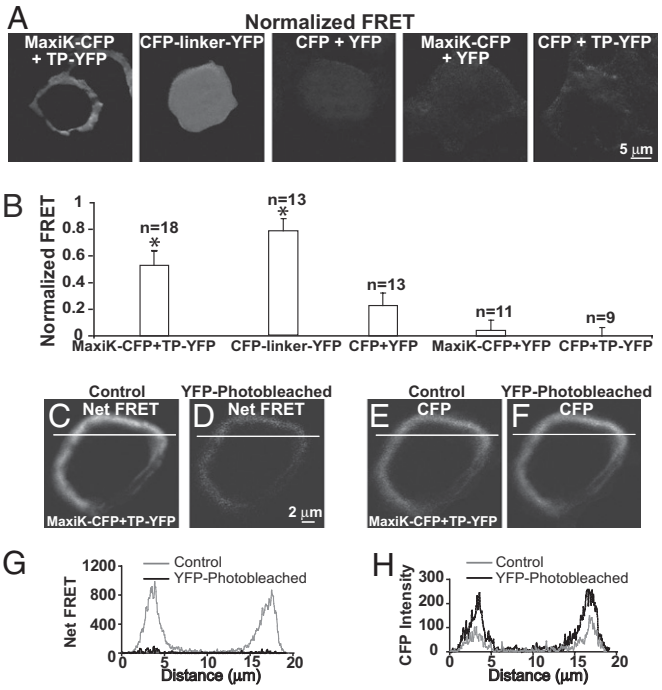

Fig. 2. FRET between MaxiK–CFP and TP–YFP. (*A*) Normalized FRET in HEK293T cells coexpressing: MaxiK–CFP + TP–YFP; positive control, CFP-linker-YFP; and negative controls, CFP + YFP, MaxiK–CFP + YFP, and CFP + TP–YFP. (*B*) Mean normalized FRET values. *Significantly different from negative controls ($P < 0.01$). (*C* and *D*) Net FRET in cells coexpressing MaxiK–CFP + TP–YFP before (control) and after photobleaching with 491-nm laser (YFP-photobleached). (*E* and *F*) MaxiK–CFP emission (excited at 405 nm and measured at 465 nm) before (control) and after photobleaching (YFP-photobleached). Lines, regions used to generate line-scan graphs showing decreased net FRET (*G*) and increased CFP (*H*) intensity after YFP photobleaching.

TP First Intracellular Loop and C Terminus Interact with MaxiK. All of the above results showing a close interplay of TP with MaxiK prompted the question, which TP domains interact with MaxiK? TP is a classical seven-transmembrane receptor (Fig. 4*A*) whose intracellular loops and carboxyl terminus play a role in signal transduction through interaction with downstream effectors. We reasoned that signaling of TP to MaxiK would most probably occur through the interaction of these domains with MaxiK. To test this possibility, recombinant GST and GST-fusion proteins containing the first (ICL1), second (ICL2), or third (ICL3) intracellular loops or the C terminus (C-ter) of TP (Fig. 4*B*) were used to pull down MaxiK from lysates of expressing HEK293T cells. GST protein complexes were immunoblotted with anti-MaxiK (Fig. 4*C*) and with anti-GST (Fig. 4*D*) antibodies, the latter to ensure proper expression. Compared with GST alone (Fig. 4*C*, lane 1), the intracellular loop 1 had a clear interaction with MaxiK (Fig. 4*C*, lane 2), whereas the C terminus exhibited a weaker but significant interaction (Fig. 4*C*, lane 5). In contrast, intracellular loop 2 (lane 3) and intracellular loop 3 (lane 4) had practically no interaction with MaxiK. Mean intensity values normalized to GST signals (Fig. 4*E*) show that the intracellular loop 1 and the C terminus of TP interact with MaxiK being fourfold (4 ± 1; $n = 3$), and near threefold (2.8 ± 0.5; $n = 3$) stronger than GST alone.

TP–MaxiK Interaction Involves MaxiK Voltage Sensing-Conduction Cassette. We next examined whether the voltage-sensing conduction cassette or the C terminus of MaxiK are involved in TP interaction. To this end, the wild-type $MaxiK_{1–1113}$ and two overlapping constructs were used: (*i*) $MaxiK_{1–711}$ containing the voltage-sensing-conduction cassette (including transmembrane segments S0–S6) and part of the C terminus, and (*ii*) $MaxiK_{322–1113}$ encompassing the whole C terminus (Fig. 4*F*). All constructs were c-Myc tagged at the N terminus and expressed in HEK293T cells. Consistent with a role of MaxiK voltage-sensing cassette, coimmunoprecipitation showed that $MaxiK_{1–1113}$ as well as $MaxiK_{1–711}$ but not $MaxiK_{322–1113}$ were able to pull down TP ($n = 3$; Fig. 4*G*, lanes 1 and 2 vs. 3). Lack of TP pull-down by $MaxiK_{322–1113}$ was not due to unfavorable immunoprecipitation of $MaxiK_{322–1113}$, as shown in Fig. 4*H*, lane 3. Verifying these data, reverse coimmunoprecipitation demonstrated that TP pulls down $MaxiK_{1–1113}$ and $MaxiK_{1–711}$ but not the C terminus ($MaxiK_{322–1113}$; Fig. 4*I*, lanes 1 and 2 vs. 3), although TP was effectively immunoprecipitated in all instances (Fig. 4*J*; $n = 3$).

To directly test the role of the voltage-sensing conduction cassette in MaxiK–TP association, we used $MaxiK_{1–343}$, which contains the voltage-sensing conduction cassette, plus the 22-aa linker to RCK1 domain (Fig. 4*F*), because the construct without linker is poorly expressed. Coimmunoprecipitation experiments demonstrate that $MaxiK_{1–343}$ readily interacts with TP only in lysates from cells expressing both proteins (Fig. 4*K*; $n = 3$). As positive control, immunoprecipitation of $MaxiK_{1–343}$ is also shown (Fig. 4*L*). Furthermore, TP intracellular loop 1 identified above as the best interacting TP intracellular domain (Fig. 4*E*) readily pulled down $MaxiK_{1–343}$ in a GST pull-down assay (Fig. S6).

The absence of MaxiK C-terminus ($MaxiK_{322–1113}$) coimmunoprecipitation signals may not preclude its possible interaction with TP, because its detection may be limited by the sensitivity of the method or by changes in conformation or targeting of the truncated construct. Supporting MaxiK C-terminus interactions, we observed FRET in MaxiK–CFP and TP–YFP C-terminal fusion proteins, and when given optimum experimental conditions, as in GST pull-down assays, we were able to observe interaction between MaxiK C terminus and the intracellular loop 1 of TP (Fig. S6). Also, immunocytochemistry shows that $MaxiK_{322–1113}$ expresses at the cell periphery, and although to a much lower degree than the wild-type channel, it is able to associate with TP with a protein proximity index of ~0.3 (Fig. S7).

In summary, the data show that MaxiK voltage-sensing conduction cassette is sufficient for the interaction of MaxiK and TP, and that MaxiK C terminus may participate in the interaction.

TP and MaxiK Channel Complex in Vascular Smooth Muscle. The relevance of TP and MaxiK complex formation in the vasculature was directly tested using human coronary arteries as well as rat aorta. In both vascular beds ($n = 6$), anti-TP antibody was able to coimmunoprecipitate MaxiK (Fig. 5 *A* and *B*, lane 2), which was recognized by the corresponding antibody at the expected molecular mass of the monomer (~125 kDa). As expected for a specific interaction, anti-rabbit IgG was unable to pull down MaxiK (Fig. 5 *A* and *B*, lane 1). In human coronaries, we could also detect a MaxiK band of ~250 kDa, which would correspond to the dimer (Fig. 5*A*, lane 2; dots). The bands near 100 kDa (lanes 1 and 2) are nonspecific, as they were also observed when immunoprecipitation was performed with anti-IgG. For reference, we also show the immunoblot of input lysates labeled with anti-MaxiK (Fig. 5 *A* and *B*, lane 3) and anti-TP (Fig. 5*C*) antibodies. For TP, a strong ~49-kDa band (blocked by the antigenic peptide; Fig. S8) was observed that can correspond to the phosphorylated or glycosylated form of the 37-kDa naïve receptor (7, 8). We also probed the aorta blot with anti–c-Src antibody. c-Src was labeled in the lysate but was not pulled down by anti-rabbit IgG nor by anti-TP antibody (Fig. 5*B*, lane 3 vs. lanes 1 and 2). The failure of anti-TP antibody to immunoprecipitate c-Src, an abundant protein in smooth muscle that partially couples to TP contractile function (9), and the negative controls showing lack of MaxiK signals with anti-rabbit IgG, strongly support the specificity of TP–MaxiK association in native tissues.

Coimmunoprecipitation of TP and MaxiK was performed with vascular tissues formed of more than one cell type, such as fibroblasts and endothelial and smooth muscle cells. To verify that the interaction of TP and MaxiK occurs in vascular myocytes and identify the subcellular regions where TP and MaxiK normally interact, human coronary myocytes were freshly isolated

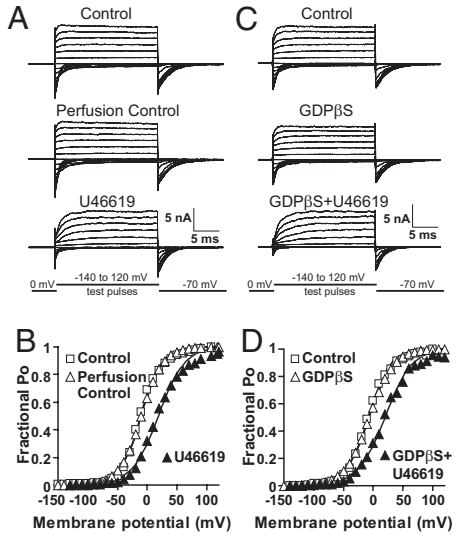

Fig. 3. GDPβS fails to prevent U46619-induced TP-mediated MaxiK channel inhibition. Inside-out patch currents in cells expressing MaxiK + TP. Holding potential = 0 mV; test pulses were from −140 to 120 mV; repolarizing pulses were to −70 mV. (*A*) Currents upon patch excision (control), 5 min after mock perfusion (perfusion control), and 15 min after 500-nM U46619 treatment (U46619). (*B*) Mean fractional open probability (Po) vs. membrane potential plots. U46619 induced a rightward shift consistent with MaxiK inhibition. (*C*) MaxiK currents upon patch excision (control), 5 min after 500 μM GDPβS and 15 min after 500 μM GDPβS plus 500 nM U46619 perfusion. (*D*) U46619 induced same rightward shift of the voltage activation curve with GDPβS as in its absence. (*B* and *D*) Instantaneous tail currents were fitted to a Boltzmann distribution to obtain $V_{1/2}$ values (*SI Materials and Methods*).

and double-immunolabeled to detect MaxiK (Fig. 5*D*, red) and TP (Fig. 5*E*, green). Experiments in permeabilized cells revealed a high degree of overlap between TP and MaxiK signals at the cell periphery (Fig. 5*F*, yellow). Supporting specific colocalization, the cross-correlation 3D plot as a function of pixel shift (Fig. 5*G*) shows a sharp peak at zero pixel shift that decays abruptly by moving the image in the *x* and *y* axes. The mean protein proximity values for TP→MaxiK of 0.52 ± 0.06 and for MaxiK→TP of 0.53 ± 0.13 (n = 6; Fig. 5*H*) indicate that in coronary myocytes about the same fraction of TP (52%) associates with MaxiK, as MaxiK (53%) to TP. Taken together, the coimmunoprecipitation and colocalization analyses show that TP and MaxiK are assembled in a physical macrocomplex at the plasma membrane of vascular myocytes.

TP Activation Inhibits MaxiK Channel in Human Coronary Arterial Myocytes. Finally, we examined whether inhibition of MaxiK channels by TP stimulation occurs in freshly dissociated human coronary myocytes. The inside-out patch clamp configuration was chosen to test MaxiK and TP close-coupling and to maintain activating Ca^{2+} as a constant parameter. MaxiK channels were exposed to GTP-free solutions and to an internal calcium concentration of 18 μM, which is within the range of the estimated Ca^{2+} that the channel senses during spontaneous Ca^{2+} sparks in cerebral arterial myocytes (10). Control recordings, and recordings following application of drugs, were taken for 7–20 min to take into account the typical oscillatory behavior of MaxiK channels. Fig. 6 *A* and *B* shows channel inhibition by U46619 (500 nM) at different voltages. The traces illustrate the robust channel inhibition induced by U46619 at a membrane voltage of −60 mV. The open probability, Po, decreased near 80% from 0.83 to 0.19. The voltage activation curve (open probability vs. voltage) fitted to a Boltzmann distribution (continuous line) shows that activation of TP by U46619 inhibits MaxiK, causing a rightward 35-mV shift with the voltage necessary to half-activate the channel, $V_{1/2}$, changing from −75 mV to −40 mV. The mean inhibitory

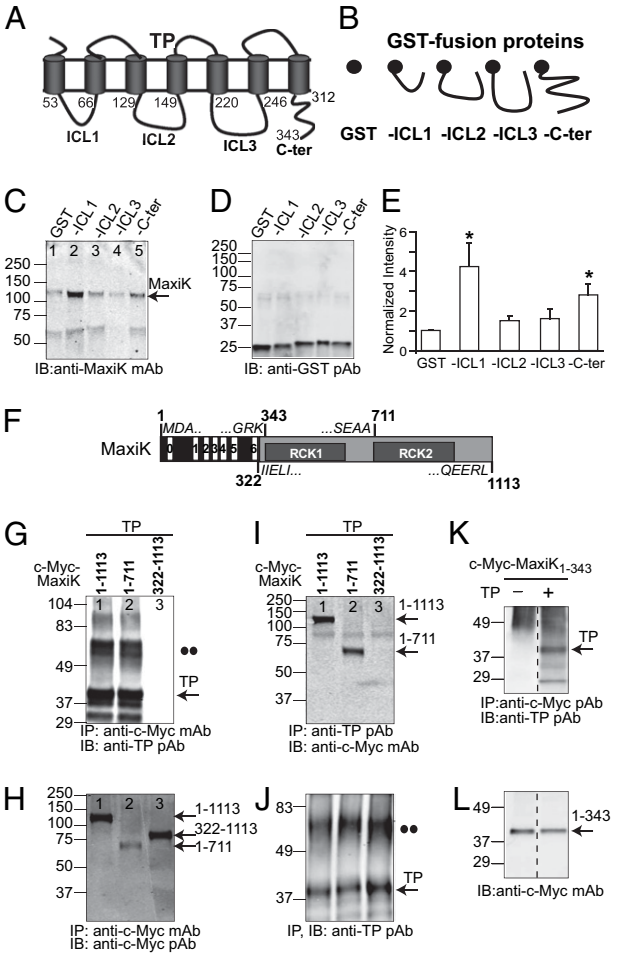

Fig. 4. Identifying TP–MaxiK association domains. (*A* and *B*) Schemes of TP, GST, and GST-fusion proteins of TP intracellular loops 1–3 (-ICL1, -ICL2, and -ICL3) and C terminus (-C-ter). Numbers correspond to amino acid residues delimiting corresponding domains. (*C*) Pull-down of MaxiK from transfected HEK293T cell lysates by purified recombinant GST or GST-fusion proteins. (*D*) Immunoblot of GST and GST-fusion proteins. (*E*) Quantification of MaxiK pull-down by TP domains. Data were normalized to GST expression in each experiment (n = 3). *Significantly different from GST control ($P < 0.05$). (*F*) Scheme of MaxiK full-length ($MaxiK_{1–1113}$). Boundaries of $MaxiK_{1–343}$, $MaxiK_{1–711}$, and $MaxiK_{322–1113}$ are marked, and flanking sequences are given. Black box, voltage-sensing conduction cassette. Gray box, intracellular C terminus. RCK1, RCK2, regulators of K conductance 1 and 2 domains. (*G*) MaxiK constructs coimmunoprecipitate TP. (*H*) Corresponding immunoprecipitation of MaxiK constructs (positive control). (*I*) TP coimmunoprecipitates MaxiK constructs. (*J*) Corresponding immunoprecipitated TP (positive control). •• indicate putative TP dimers (*G* and *J*). (*K*) $MaxiK_{1–343}$ coimmunoprecipitates TP. (*L*) Corresponding immunoprecipitated $MaxiK_{1–343}$ (positive control). Dashed lines, an unrelated middle lane was omitted.

action by U46619 on MaxiK channel activity at −60 mV is shown in the inset.

We next examined whether TP mediates thromboxane A2-induced MaxiK channel inhibition by testing the action of the TP antagonist SQ29,548. Fig. 6*C* illustrates an inside-out patch at 0 mV containing three MaxiK channels. In control conditions, the channels were most of the time open. After U46619 (500 nM) treatment, long closings were produced, which were reversed by the simultaneous perfusion of SQ29,548 (5 μM). To quantify the effect of the TP antagonist, the time course of channel Po was plotted. For illustration purposes, the diary plot shows representative segments of channel activity during the experiment that lasted a total of 86 min. In control conditions,

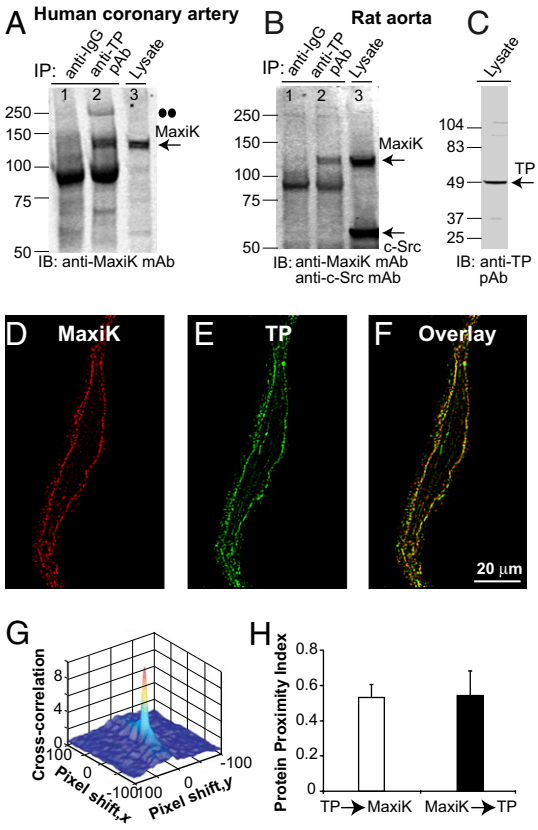

Fig. 5. Vascular TP and MaxiK form a protein complex. (*A* and *B*) TP coimmunoprecipitates MaxiK in lysates of human coronary arteries and rat aorta (lane 2). Anti-rabbit IgG does not coimmunoprecipitate MaxiK (lane 1). (*A* and *B*, lane 3, and *C*) Input coronary and aorta lysates (40 and 50 μg protein, respectively). Double dots mark putative MaxiK dimer. (*D* and *E*) Freshly dissociated human coronary arterial myocyte double-labeled with anti-MaxiK monoclonal (red) and anti-TP polyclonal (green) antibodies. (*F*) Overlay (yellow). Images at 0.0288 μm/pixel after median filter background reduction. (*G*) TP and MaxiK 3D cross-correlation plot as a function of pixel shift. (*H*) Mean values of protein proximity index.

MaxiK channel had a mean Po of about 0.8. Ten minutes after U46619 treatment (arrow), channel activity decreased to a steady Po of around 0.4 that lasted >25 min. Reversion by SQ29,548 (5 μM) to a Po of 0.88 was completely established 30 min after application of the drug and was maintained for the duration of the experiment. Recovery by SQ29,548 was observed in another two experiments confirming the role of TP in U46619-mediated inhibition of MaxiK channels.

Discussion

We showed the regulation and physical association of MaxiK channel with TP, a vasoconstricting GPCR. TP and MaxiK form a multimeric complex in close proximity (within 6 nm distance), providing a spatial context that facilitates TP-induced *trans*-inhibition of MaxiK without the necessity of G-protein signaling.

Interaction of TP and MaxiK and Its Molecular Mechanisms. GPCR interacting proteins (GIPs) help transduce GPCR activation to intracellular signaling pathways. The vast majority of GIPs are intracellular proteins; a classical example are the arrestins, which act as multiprotein scaffolds, helping recruit signaling proteins to GPCRs and allowing GPCRs to function independently of G-protein activation (11). Intracellular GIPs have been identified for the long β-isoform of TP, e.g. the small Rab11 GTPase, whose function is related to TP traffic mechanisms (12). In contrast, identification of transmembrane GIPs has been seldom and circumscribed to either GPCR dimerization or to dopamine receptors and ionotropic $GABA_A$ and NMDA receptors. The latter use direct protein–protein interactions demonstrated biochemically (13, 14) or supported spectroscopically (15).

We now provide evidence for a voltage-gated ion channel (MaxiK) in direct interaction with a GPCR, in this case the TP receptor. MaxiK–TP multimeric structure most likely enables MaxiK to act as a direct downstream effector of TP in the vasculature and possibly other systems. A direct protein–protein interaction between TP and MaxiK is strongly supported by the fact that MaxiK–CFP and TP–YFP C-termini are ∼6 nm apart, as evaluated by FRET experiments. Additional evidence for this idea are the TP-induced MaxiK inhibition independent of G-protein activation as well as the coimmunoprecipitation and protein proximity analyses showing that TP and MaxiK constitutively assemble in a physical complex along the plasmalemma of vascular myocytes.

The TP first intracellular loop and, to a lesser extent, its C terminus, interact with full-length MaxiK, whereas the voltage-sensing conduction cassette lacking the intracellular C terminus (first N-terminal third of MaxiK) is sufficient for the interaction with full-length TP. These molecular data indicate that TP–MaxiK physical interaction involves mainly the first intracellular loop and C terminus of TP and the N-terminal intracellular loops of MaxiK. A potential role of MaxiK C terminus is supported by FRET, immunocytochemistry, and in vitro pull-down results. All of the above interactions could mediate conformational rearrangements in MaxiK, leading to its inhibition.

Regulation of MaxiK Channel by Vasoconstrictor TP Receptor. Previous studies reporting thromboxane A2 (U46619) and angiotensin II mediated inhibition of vascular MaxiK channel in lipid bilayers proposed the potential role of these vasoconstrictors on MaxiK regulation in the vasculature (5, 16). Our findings provide

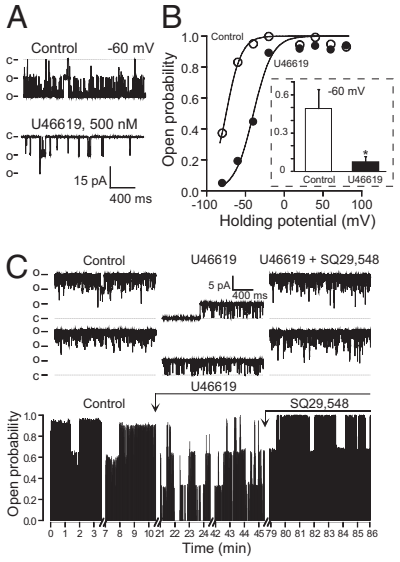

Fig. 6. TP agonist U46619 inhibits MaxiK channel activity in human coronary arterial myocytes through activation of TP receptor. (*A*) Inside-out channel traces before (control) and after inhibition with 500 nM U46619 at −60 mV. Pipette and bath solution was (in mM): 140 K-methanesulfonate (KMes), 2 $MgCl_2$, 10 Hepes, 10 glucose, 0.005 $CaCl_2$, pH 7.4, pCa 4.74. (*B*) U46619 causes a rightward shift of the voltage activation curve. Data were fitted to a Boltzmann distribution. (*Inset*) Mean open probability at −60 mV (control, $n = 5$; U46619, $n = 4$). *Significantly different, $P < 0.05$. (*C Upper*) Traces of MaxiK channel activity at 0 mV before (control), after U46619 (500 nM) inhibition, and reversal by cotreatment with TP antagonist SQ29,548 (5 μM). (*Lower*) Diary plot. Mean open probability changed from 0.8 (control) to 0.4 after U46619, and recovered to 0.88 with SQ29,548. Pipette solution (in mM): 135 NaMes, 5 KMes, 2 $MgCl_2$, 1.8 $CaCl_2$, 10 Hepes, 10 glucose, pH 7.4. Bath solution as in *A*. o, open state; c, closed state.

evidence for vasoconstrictor TP receptor physical association with MaxiK channels, resulting in channel inhibition after agonist stimulation in living arterial smooth muscle.

GPCRs classically transduce signals through G-protein–dependent mechanisms; however, G-protein–independent pathways can also take place. G-protein (both α and βγ)–dependent mechanisms are known to modulate MaxiK channel activity by a handful of GPCRs. For example, G-protein α-subunits (α_s, $\alpha_{i/o}$) are involved in MaxiK channel regulation by β-adrenergic and muscarinic receptors (2, 3) in smooth muscle. Likewise, G-protein βγ-dimer also mediates M_2 muscarinic receptor-induced MaxiK channel inhibition (17). G-protein activation requires guanine nucleotide exchange, which switches the G protein from its inactive GDP-bound state to its active GTP-bound state. In our study, we found that G-protein activation is not required for TP-mediated MaxiK channel inhibition, as this process was observed in the presence of GDPβS (which favors the inactive GDP bound state) as well as in the absence of GTP in inside-out patches. Interestingly, in chromaffin cells, μ-opioid receptors have been observed to activate MaxiK channel activity in the presence of GDPβS (18). Thus, GPCRs may directly regulate MaxiK activity; in the case of TP by inhibiting its activity via a mechanism that is independent of G-protein signaling, likely entailing protein–protein crosstalk.

MaxiK channels are regulated by protein kinases involving direct phosphorylation of the channel. Protein kinases such as PKA, PKG, PKC, and c-Src are known to regulate MaxiK channel activity (19–22). In all these cases, channel phosphorylation requires ATP as phosphoryl donor and occurs in conditions that have either endogenous ATP (cell attached or whole-cell patch recordings) or exogenous ATP (inside-out recording). In our experiments, inhibition of MaxiK by U46619 using inside-out patches without ATP supports the view that in this case MaxiK inhibition does not result from channel phosphorylation or secondary intracellular signaling pathways mediated by protein phosphorylation.

In the present studies, U46619 (for 100 nM, see Fig. S9; for 500 nM, see Figs. 3 and 6) could inhibit MaxiK channel activity by perfusing the drug to the intracellular side of inside-out patches. U46619 could traverse the membrane to reach its receptor at the extracellular side of the membrane because the TP receptor antagonist SQ29,548 could reverse U46619 effect (Fig. 6*C*). However, in bilayers, 100-nM U46619 inhibited channel activity only when added to the extracellular side of the channel (5). This difference in U46619 membrane permeability between bilayers and cell studies may be due to the presence of decane and a different lipid composition of black lipid bilayers with respect to the natural membrane composition of HEK293T cells and human coronary myocytes.

Recently, Lu et al. (23) showed that angiotensin II is also able to inhibit MaxiK channel activity in rat coronary arterial myocytes, and that this regulation was absent during diabetes. These findings, together with the work presented here, highlight the functional and physical relationship between MaxiK and vasoconstrictor receptors, opening the possibility of MaxiK involvement in vasoconstricting events.

Materials and Methods

Detailed procedures can be found in *SI Materials and Methods*.

Animals. Three-month-old male rats (Sprague–Dawley) were used. Protocols received institutional approval.

Coronary Arterial Myocytes. Human coronary arteries were collected from explanted hearts at the UCLA Medical Center. All procedures received institutional review board approval. Cells were enzymatically dissociated.

Patch Recording. MaxiK channel activity was recorded in inside-out patches. In HEK293T cells, currents were recorded ~24 h after transfection with TP and MaxiK in pIRES vector.

Biochemistry, Imaging, and Colocalization Analysis. Immunochemistry of tissues or transfected cells and GST pull-down assays were by standard procedures. Confocal sections were acquired every 0.1–0.2 μm (*z* axis) at 0.0288 or 0.057 μm/pixel. Protein proximity index was calculated at the middle of cells (6).

FRET. Fixed cells and a custom-made high-resolution confocal microscope were used. Each set of experiments were performed at constant laser intensities and photomultiplier gains.

Statistics. Data are means ± SD. Statistical comparisons were made using Student's *t* test. A P value < 0.05 was considered statistically significant.

ACKNOWLEDGMENTS. This work was supported by National Institutes of Health Grants HL096740 (to E.S. and L.T.), HL088640 (to E.S.), and HL54970 (to L.T.), and American Heart Association Postdoctoral Fellowship 0825273F (to M.L.).

1. Toro L, Ramos-Franco J, Stefani E (1990) GTP-dependent regulation of myometrial KCa channels incorporated into lipid bilayers. *J Gen Physiol* 96:373–394.
2. Kume H, Graziano MP, Kotlikoff MI (1992) Stimulatory and inhibitory regulation of calcium-activated potassium channels by guanine nucleotide-binding proteins. *Proc Natl Acad Sci USA* 89:11051–11055.
3. Scornik FS, Codina J, Birnbaumer L, Toro L (1993) Modulation of coronary smooth muscle KCa channels by Gs alpha independent of phosphorylation by protein kinase A. *Am J Physiol* 265:H1460–H1465.
4. Liu G, et al. (2004) Assembly of a Ca2+-dependent BK channel signaling complex by binding to beta2 adrenergic receptor. *EMBO J* 23:2196–2205.
5. Scornik FS, Toro L (1992) U46619, a thromboxane A2 agonist, inhibits KCa channel activity from pig coronary artery. *Am J Physiol* 262:C708–C713.
6. Wu Y, et al. (2010) Quantitative determination of spatial protein-protein correlations in fluorescence confocal microscopy. *Biophys J* 98:493–504.
7. Wang GR, Zhu Y, Halushka PV, Lincoln TM, Mendelsohn ME (1998) Mechanism of platelet inhibition by nitric oxide: In vivo phosphorylation of thromboxane receptor by cyclic GMP-dependent protein kinase. *Proc Natl Acad Sci USA* 95:4888–4893.
8. Kelley LP, Kinsella BT (2003) The role of N-linked glycosylation in determining the surface expression, G protein interaction and effector coupling of the alpha (alpha) isoform of the human thromboxane A(2) receptor. *Biochim Biophys Acta* 1621:192–203.
9. Lu R, et al. (2008) c-Src tyrosine kinase, a critical component for 5-HT2A receptor-mediated contraction in rat aorta. *J Physiol* 586:3855–3869.
10. Pérez GJ, Bonev AD, Patlak JB, Nelson MT (1999) Functional coupling of ryanodine receptors to KCa channels in smooth muscle cells from rat cerebral arteries. *J Gen Physiol* 113:229–238.
11. DeWire SM, Ahn S, Lefkowitz RJ, Shenoy SK (2007) Beta-arrestins and cell signaling. *Annu Rev Physiol* 69:483–510.
12. Thériault C, Rochdi MD, Parent JL (2004) Role of the Rab11-associated intracellular pool of receptors formed by constitutive endocytosis of the beta isoform of the thromboxane A2 receptor (TP beta). *Biochemistry* 43:5600–5607.
13. Liu F, et al. (2000) Direct protein-protein coupling enables cross-talk between dopamine D5 and gamma-aminobutyric acid A receptors. *Nature* 403:274–280.
14. Lee FJ, et al. (2002) Dual regulation of NMDA receptor functions by direct protein-protein interactions with the dopamine D1 receptor. *Cell* 111:219–230.
15. Fiorentini C, Gardoni F, Spano P, Di Luca M, Missale C (2003) Regulation of dopamine D1 receptor trafficking and desensitization by oligomerization with glutamate N-methyl-D-aspartate receptors. *J Biol Chem* 278:20196–20202.
16. Toro L, Amador M, Stefani E (1990) ANG II inhibits calcium-activated potassium channels from coronary smooth muscle in lipid bilayers. *Am J Physiol* 258:H912–H915.
17. Zhou XB, et al. (2008) M2 muscarinic receptors induce airway smooth muscle activation via a dual, Gbetagamma-mediated inhibition of large conductance Ca2+-activated K+ channel activity. *J Biol Chem* 283:21036–21044.
18. Twitchell WA, Rane SG (1994) Nucleotide-independent modulation of Ca(2+)-dependent K+ channel current by a mu-type opioid receptor. *Mol Pharmacol* 46:793–798.
19. Robertson BE, Schubert R, Hescheler J, Nelson MT (1993) cGMP-dependent protein kinase activates Ca-activated K channels in cerebral artery smooth muscle cells. *Am J Physiol* 265:C299–C303.
20. Sadoshima J, Akaike N, Kanaide H, Nakamura M (1988) Cyclic AMP modulates Ca-activated K channel in cultured smooth muscle cells of rat aortas. *Am J Physiol* 255: H754–H759.
21. Lange A, Gebremedhin D, Narayanan J, Harder D (1997) 20-Hydroxyeicosatetraenoic acid-induced vasoconstriction and inhibition of potassium current in cerebral vascular smooth muscle is dependent on activation of protein kinase C. *J Biol Chem* 272: 27345–27352.
22. Alioua A, et al. (2002) Coupling of c-Src to large conductance voltage- and Ca2+-activated K+ channels as a new mechanism of agonist-induced vasoconstriction. *Proc Natl Acad Sci USA* 99:14560–14565.
23. Lu T, et al. (2010) Regulation of coronary arterial BK channels by caveolae-mediated angiotensin II signaling in diabetes mellitus. *Circ Res* 106:1164–1173.